Article

pubs.acs.org/Biomac

Diepoxide-Triggered Conformational Transition of Silk Fibroin: Formation of Hydrogels

Ilknur Karakutuk, Fatih Ak, and Oguz Okay*

Istanbul Technical University, Department of Chemistry, 34469 Istanbul, Turkey

Supporting Information

ABSTRACT: Silk fibroin hydrogels with tunable properties could be obtained from aqueous fibroin solutions (4.2 w/v %) in a short period of time. This was achieved by the addition of ethylene glycol diglycidyl ether (EGDE) into the reaction solution. Introduction of EGDE cross-links between the fibroin molecules decreases the mobility of the chains, which triggers the conformational transition from random-coil to β-sheet structure and hence fibroin gelation. Dynamic rheological measurements conducted at 50 °C show the formation of strong to weak hydrogels depending on the pH of the reaction solution. Although EGDE attacks the amino groups of fibroin and forms interstrand cross-links, β-sheets acting as physical cross-links dominate the elasticity of the hydrogels. Mechanical response of low-modulus fibroin hydrogels formed above pH 9.7 is highly nonlinear with strong strain hardening behavior (700%) arising from the alignment of the crystallizable amino acid segments.

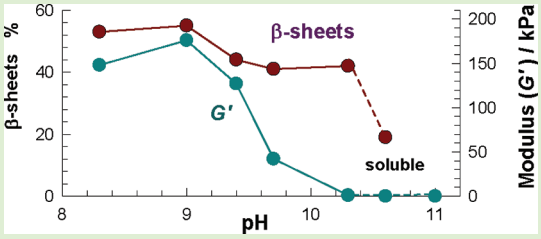

INTRODUCTION

Silk fibroin derived from *Bombyx mori* is a fibrous protein exhibiting unique material properties including good biocompatibility, biodegradability, high strength and toughness, and versatility in processing.[1−3] Silk fibroin has a multiblock polymer architecture consisting of large hydrophobic and smaller hydrophilic internal blocks together with large hydrophilic chain end blocks.[4−7] Hydrophilic blocks of fibroin provide solubility in water, whereas associations between the hydrophobic blocks induce a conformation transition from random-coil or helix to β-sheet structure. The presence of β-sheets in silk fibroin is responsible for its high strength, whereas the less ordered hydrophilic blocks give rise to its elasticity and toughness. Many factors such as fibroin concentration,[8,9] pH,[8−16] temperature,[8,9] metallic ions,[8,12,15−22] dielectric constant of solvent,[23] electric field,[24,25] and shearing[26] (spinning) facilitate the conformation transition in silk fibroin molecules.

Intermolecular β-sheets in fibroin solutions acting as physical cross-link zones lead to the formation of hydrogels, which are stable under physiological conditions. However, as compared with many protein gels, rate of fibroin gelation in homogeneous aqueous solutions is unusually slow. For example, 1 to 7% aqueous solutions of silk fibroin at 37 °C undergo sol−gel transition after 5 to 7 days.[9] As the pH of the solution is increased beyond 9, the gelation time further increases, and at pH 10, gelation occurs after about 1 month.[9] This long gelation time is due to the osmotic pressure of the counterions of carboxyl groups on fibroin molecules causing chain expansion and reducing the extent of hydrophobic interactions. In acidic pH, because the carboxyl groups are in nonionized form, fibroin molecules assume a smaller size in aqueous solutions,[27] which promotes β-sheet formation. However, even at pH near the isoelectric point (pI = 3.8 to 3.9), the gelation of 3% fibroin solution occurs within 2 days.[28]

Herein, we report that gelation of aqueous silk fibroin solutions (4.2 w/v %) in the presence of ethylene glycol diglycidyl ether (EGDE) leads to the formation of hydrogels with a wide range of tunable properties. EGDE has been widely used for cross-linking of polysaccharides, proteins, DNA, as well as organic molecules.[29−32] EGDE contains epoxide groups on both ends that can react with nucleophiles, including amino groups, sulfhydryls, and hydroxyls. Dynamic rheological measurements performed during the solution cross-linking of fibroin at 50 °C show the formation of strong to weak hydrogels in a short period of time. The elastic modulus of fibroin hydrogels formed between pH 8.3 and 9.7 is more than two orders of magnitude larger than the modulus of chemical or other biological gels due to the conformational transition in fibroin from random-coil to β-sheet structures. Low-modulus fibroin hydrogels formed at higher pH exhibit strong strain hardening behavior due to the alignment of the crystallizable amino acid domains in silk fibroin. Such a strong chain stiffening under strain was previuosly observed in many biological gels consisting of semiflexible filaments,[33−37] which provides their tissue integrity to overcome the external forces.

EXPERIMENTAL PART

Materials. Cocoons of *Bombyx mori* were kindly provided from Koza Birlik (Agriculture Sales Cooperative for Silk Cocoon, Bursa, Turkey). Silk fibroin solution was prepared following Kim et al.'s procedure.[8] The cocoons were cut into smaller pieces and placed in 1 L of boiling aqueous solution of 0.02 M Na_2CO_3 for 1 h to remove

Received: January 3, 2012
Revised: February 10, 2012
Published: February 23, 2012

sericins. Then, silk fibers were rinsed three times in 1 L of distilled water at 70 °C for 20 min each. The extracted silk fibroin was dissolved in a 9.3 M LiBr solution at 60 °C for 4 h, yielding a 20 w/v % solution. This solution was dialyzed using dialysis tubing (10 000 MWCO, Snake Skin, Pierce) for 3 days against water that was changed three times a day. After centrifugation, the final concentration of the silk fibroin aqueous solution was about 5 w/w %, which was determined by weighing the remaining solid after drying.

The cross-linker EGDE (50%, technical grade, Fluka), *N,N,N′,N′*-tetramethylethylenediamine (TEMED, Merck), Na_2CO_3, LiBr, acetic acid (all from Merck), glucose (Fluka), and glycine (Fluka) were used as received. The cross-linker content of the reaction solution was expressed as EGDE %, the volume of pure EGDE added per 100 g of silk fibroin.

Gelation Reactions. The reactions were carried out in aqueous fibroin solutions at 50 °C in the presence of EGDE cross-linker and TEMED catalyst. The concentration of silk fibroin was fixed at 4.2 w/v % throughout the experiments, while the amount of TEMED was varied between 0 and 0.50 v/v %. To illustrate the synthetic procedure, we give details for the preparation of hydrogels with 150% EGDE: 5 mL of the aqueous fibroin solution (5 w/w %) was mixed with EGDE (0.752 mL corresponding to 0.376 mL pure EGDE or 5.0 mmol epoxy groups) and 0.248 mL of aqueous TEMED of various concentrations. Although the addition of EGDE did not change pH of the fibroin solution, TEMED changed significantly (Figure S1 of the Supporting Information). Increasing amount of TEMED from 0 to 0.50 v/v % also increased the pH of the reaction solution from 5.7 to 11.0. For the rheological experiments, a portion of the homogeneous reaction solution was transferred within the rheometer, whereas the remaining part was transferred into several plastic syringes of 4 mm internal diameters. The syringes were placed in an oven at 50 °C to conduct the cross-linking reactions for 1 day.

Determination of the Amine Group Content on Fibroin. The primary amine group content of silk fibroin during the cross-linking reactions up to the onset of gelation was monitored using 2,4,6-trinitrobenzene sulfonic acid (TNBS) method.[38,39] TNBS reacts specifically with the amino groups in silk fibroin to form a highly chromogenic trinitrophenyl derivative, whose absorbance is related to the amount of the free amino groups. Samples of 50 μL were withdrawn from the reaction solution at different times, and they were diluted to 1 mL using 0.1 M $NaHCO_3$ (pH 8.9). The solution was then mixed with 0.50 mL of 0.01 w/w % TNBS solution for 45 s at 500 rpm and incubated at 37 °C for 2 h. After the addition of 10% aqueous sodium dodecyl sulfate solution (0.50 mL), 1 M HCl (0.25 mL), and water (1 mL), the absorbance A_{335} was measured at 335 nm using T80 UV−visible spectrophotometer. Fibroin solutions of various concentrations were used as standards. Assuming that 1 g of silk fibroin contains 0.1 mmol free amino groups,[40] a calibration curve was prepared by plotting the concentration of free amino groups against A_{335} (Figure S2 of the Supporting Information). The fraction of the amino groups reacted at time t was calculated as $1 - C_{NH_2,t}/C_{NH_2,t=0}$, where $C_{NH_2,t}$ and $C_{NH_2,t=0}$ are the concentrations of the amino groups at time t and at $t = 0$, respectively.

Rheological Experiments. Gelation reactions were carried out at 50 °C within the rheometer (Gemini 150 Rheometer system, Bohlin Instruments) equipped with a cone-and-plate geometry with a cone angle of 4° and diameter of 40 mm. The instruments was equipped with a Peltier device for temperature control. During all rheological measurements, a solvent trap was used to minimize the evaporation. Furthermore, the outside of the upper plate was covered with a thin layer of low-viscosity silicone oil to prevent evaporation of solvent. A frequency of $\omega = 1$ Hz and a deformation amplitude $\gamma_o = 0.01$ were selected to ensure that the oscillatory deformation is within the linear regime. After 4 h, frequency-sweep tests at $\gamma_o = 0.01$ were carried out at 25 °C over the frequency range 10^{-2} to 10^{1} Hz. Silk fibroin hydrogels formed within the rheometer were subjected to stress-relaxation experiments at 25 °C. An abrupt shear deformation of controlled strain amplitude, γ_o, was applied to the gel samples, and the resulting stress $\sigma(t, \gamma_o)$ was monitored as a function of time. Here we report the relaxation modulus $G(t, \gamma_o)$ as functions of the relaxation time t and strain amplitude γ_o. The experiments were conducted with increasing strain amplitudes γ_o from 0.01 to 10. For each hydrogel, stress-relaxation experiments at various γ_o were conducted starting from a value of the relaxation modulus deviating <10% from the modulus measured at $\gamma_o = 0.01$.

Swelling and Gel Fraction Measurements. Silk fibroin hydrogels were taken out of the syringes, and they were cut into specimens of ∼10 mm in length. Each gel sample was placed in an excess of water at 24 °C, and water was replaced every other day over a period of at least for 1 month to wash out the soluble fibroin and the unreacted cross-linker. The swelling equilibrium was tested by weighing the gel samples. Then, the equilibrium swollen gel samples were immediately frozen at −25 °C for 1 day before being freeze-dried at −40 °C/0.12 mbar for 2 days and −60 °C/0.01 mbar for an additional 1 day. The freeze-drying system was made up of a freeze-dryer (Christ Alpha 2−4 LD plus) connected to a vacuum pump (Vacuubrand RZ 6). The freeze-drying pressures were adjusted using a valve controller and monitored by an active digital controller. All gels were freeze-dried under the same conditions. The water content of freeze-dried samples was determined by Karl Fischer titration (Mettler Toledo DL 38). Independent of the preparation conditions, the average water content of the samples was 3 ± 2%. The equilibrium weight swelling ratio (q_w) was calculated using the following equation

$$q_w = (m_{sw}/m_{dry}) \tag{1}$$

where m_{sw} and m_{dry} are the weights of gels after equilibrium swelling and after drying, respectively. The gel fraction W_g defined as the amount of cross-linked (water insoluble) fibroin network obtained from 1 g of fibroin was calculated as

$$W_g = \frac{m_{dry}}{m_o C_0} \tag{2}$$

where m_o is the weight of gels after preparation and C_0 is the initial concentration of fibroin in the reaction solution.

Elasticity Tests. Uniaxial compression measurements were performed on equilibrium swollen gels in water. The stress−strain isotherms were measured by using an apparatus previously described.[41,42] In brief, cylindrical gel sample (diameter 4 mm, length 7 mm) was placed on a digital balance (Sartorius BP221S). A load was transmitted vertically to the gel through a rod fitted with a PTFE end-plate. The force acting on the gel was calculated from the reading of the balance, whereas the resulting deformation was measured using a digital comparator (IDC type Digimatic Indicator 543-262, Mitutoyo Co.), which was sensitive to displacements of 10^{-3} mm. The force and the resulting deformation were recorded after 10 s of relaxation. The measurements were conducted up to ∼20% compression with increments of ca. 1%. The elastic modulus G_{sw} was determined from the initial slope of linear dependence

$$\sigma = G_{sw}(\alpha - \alpha^{-2}) \tag{3}$$

where σ is the force acting per unit cross-sectional area of the undeformed gel specimen and α is the deformation ratio (deformed length/initial length). At least three gel samples prepared at the same pH were tested for reproducibility, and the values were averaged to obtain the reported results.

X-ray Diffraction. X-ray diffraction of freeze-dried samples was obtained with Ni-filtered Cu Kα radiation ($\lambda = 0.15418$ nm) from a Shimadzu XRD-6000 X-ray generator operating at 40 kV and 30 mA. Diffraction intensity was measured in reflection mode at a scanning rate of 0.6°/min for $2\theta = 5-35°$.

ATR-FTIR Measurements. Spectra of the freeze-dried fibroin hydrogel samples were collected using a single-bounce diamond attenuated total refractance (ATR) module on a Fourier transform infrared (FTIR) spectrometer (Nicolet Nexus 6700) equipped with a liquid-nitrogen-cooled mercury−cadmium−telluride (MCT) detector. The resolution of each spectrum was 4 cm^{-1}, and 64 interferograms were coadded in the range of 500−4000 cm^{-1}. To estimate the conformation of fibroin network chains, we analyzed the spectra using

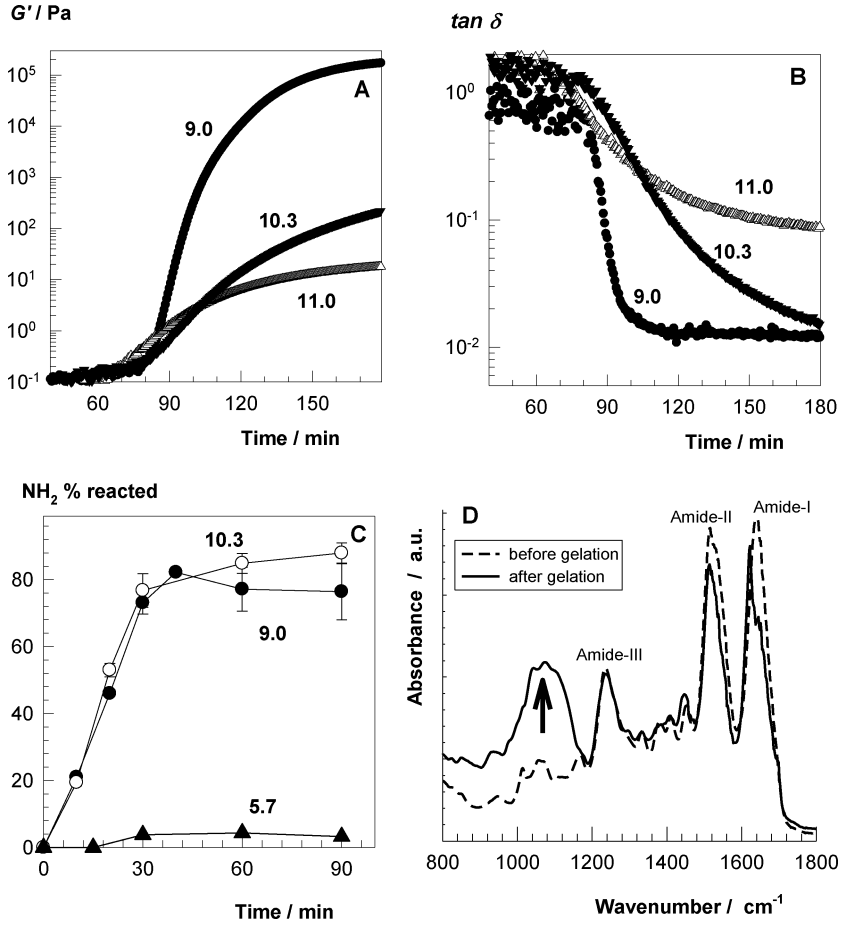

Figure 1. (A,B) Elastic modulus G' (A) and the loss factor tan δ (B) during the cross-linking of silk fibroin at 50 °C. EGDE = 150%. pH values indicated. ω = 1 Hz. γ_o = 0.01. (C) Fraction of the reacted amino groups in silk fibroin shown as a function of the reaction time. pH values indicated. (D) Typical ATR-FTIR spectra of freeze-dried silk fibroin before the reaction (dashed curve) and after gelation (solid curve). pH 10.3.

PeakFit software (version 4.12, SeaSolve Software). Linear baseline correction was applied to the amide I region (1580−1720 cm^{-1}) before the band was deconvolved by Gauss Amplitude function. For the curve fitting procedure, the initial band positions at 1620, 1640, 1660, and 1698 cm^{-1} were fixed, allowing their widths and heights to vary (Figure S3 of the Supporting Information).

RESULTS AND DISCUSSION

Silk Fibroin Gelation. Gelation of aqueous silk fibroin solutions (4.2 w/v %) was studied at 50 °C and at various pH values between 6 and 11, which was adjusted by the addition of TEMED catalyst. In the absence of EGDE and over the whole range of pH, no gel formation was observed within 1 day, whereas EGDE addition resulted in the formation of viscoelastic gels within 2 h. Increasing amount of EGDE also increased the elastic modulus of fibroin hydrogels until a limiting value at 150% EGDE was attained, corresponding to 20 mmol epoxy groups per gram of silk fibroin or 200 epoxy groups per free amino group on fibroin (Figure S4 of the Supporting Information). This value was fixed in the following experiments. To find out the functional groups on silk fibroin that are responsible for gelation, we conducted the reactions at pH 9 in the presence of three model chemicals, namely, glucose, glycine, and sodium acetate containing hydroxyl, amine, and carboxyl functional groups, respectively. Whereas the presence of glucose or sodium acetate in the reaction solution did not change the moduli of the hydrogels, the addition of glycine inhibited cross-linking reactions significantly, implying that the amine groups on fibroin are responsible for the cross-linking reactions with EGDE. Indeed, the number of the primary amine groups on fibroin decreased during the gelation process, as determined by TNBS method.

Typical gelation profiles at three different pH values are shown in Figure 1A,B, where the elastic modulus G' and the loss factor tan δ are plotted as a function of the reaction time. Gelation of silk fibroin is characterized by an initial lag phase of ~70 min, during which the dynamic moduli remain almost unchanged. The lag phase is followed by a log phase during which G' increases rapidly while tan δ decreases; then, they approach plateau values after ~3 h.

In Figure 1C, the fraction of the reacted amino groups on silk fibroin is plotted against the reaction time. At pH 5.7, the amino groups on fibroin do not react with EGDE. Indeed, no gel formation was observed at this pH value. At higher pH values, ~80% of the amino groups react within the first hour of the reaction, whereas at longer times up to the gelation point no change in the amine group content was observed. The reaction between EGDE and fibroin was also assessed by the ATR-FTIR spectra of freeze-dried fibroin samples (Figure 1D). In addition to the characteristic amide I, II, and III absorption bands, new bands at 1040−1100 cm^{-1} appear upon gelation, which were assigned to the ether stretching bands of EGDE cross-linkages.[43−45] On the basis of these measurements, we conclude that the reaction between the amine groups on fibroin

dx.doi.org/10.1021/bm300006r | Biomacromolecules 2012, 13, 1122−1128

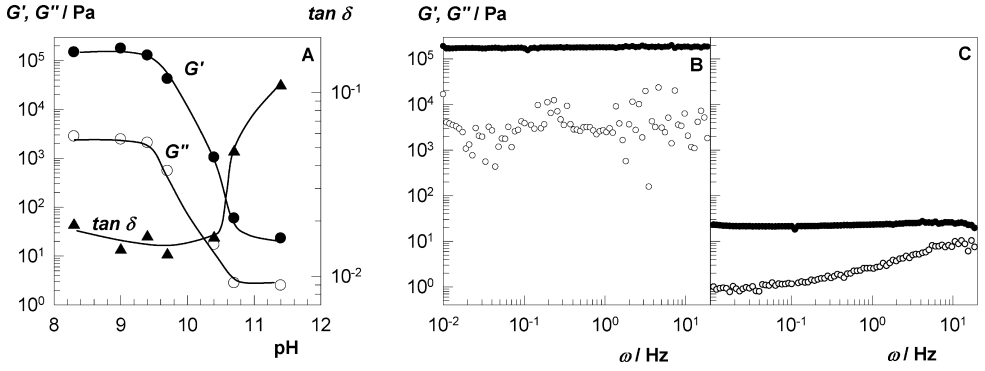

Figure 2. (A) G' (●), G'' (○), and tan δ (▲) after a reaction time of 4 h plotted against pH. (B,C) G' (●) and G'' (○) shown as a function of the frequency ω at 25 °C. γ_o = 0.01 (1%). pH 9.0 (B) and 11.0 (C).

molecules and EGDE occurs during the lag phase of the gelation reactions. Elastically effective cross-link zones between fibroin molecules leading to an increase in the elastic modulus appear much later. As will be seen later, this is due to the formation of β-sheet structures induced by EGDE cross-links.

Figure 2A shows the limiting values of G', viscous modulus G'', and tan δ after a reaction time of 4 h as a function of pH. No gel formation was observed in the absence of TEMED, that is, at pH 5.7, whereas the addition of just 0.07% TEMED into the reaction solution increases pH from 5.7 to 8.3 and leads to a marked increase in both G' and G''. Between pH 8.3 and 9.7, G' is ~10^2 kPa, which is two orders of magnitude larger than the elastic modulus reported for chemical or cross-linked biopolymer gels including actin, fibrin, agarose, and lysozyme[46,47] as well as solution cross-linked DNA hydrogels using EGDE cross-linker.[31,32] This implies that not only chemical cross-links but also conformational changes in silk fibroin contribute to the rubber elasticity of the gel network. Both G' and G'' decrease steeply, whereas the loss factor increases when pH increases from 9.7 to 11 due to the decreasing crystallinity in the hydrogels (see below). In this range of pH, the elastic modulus of the hydrogels can easily be tuned between 10^5 and 10^1 Pa by simply changing pH of the reaction medium. The results of the frequency sweep tests shown in Figure 2B,C illustrate that G' is one to two orders of magnitude larger than G'', and they are both essentially independent of frequency indicating very long relaxation time of the fibroin network chains.

Swelling and Elastic Properties. Fibroin gels in cylindrical form of 4 mm in diameter were prepared by conducting the gelation reactions at 50 °C for 1 day at various pH values between pH 8.3 and 11.0. All gel samples were translucent, indicating the existence of scattering centers for light. Figure 3A shows the equilibrium weight swelling ratio q_w and the gel fraction W_g of the hydrogels plotted against pH of the reaction solution. In accord with the viscoelastic data, q_w rapidly increases, whereas W_g decreases above pH 9.7 due to the decreasing elastic modulus of the gels (Figure 2A), and they become soluble in water at pH >10.3. The moduli of the swollen gels were investigated by the compression tests. The initial slope of the stress−strain curves (eq 3) corresponding to the shear moduli G_{sw} of the hydrogels is collected in Figure 3B. G_{sw} shows similar trend as the elastic modulus G' but with four to six times smaller values at pH values below 10 due to the dilution of the network chains. A rough estimate using the theory of rubber elasticity gives the network mesh size in

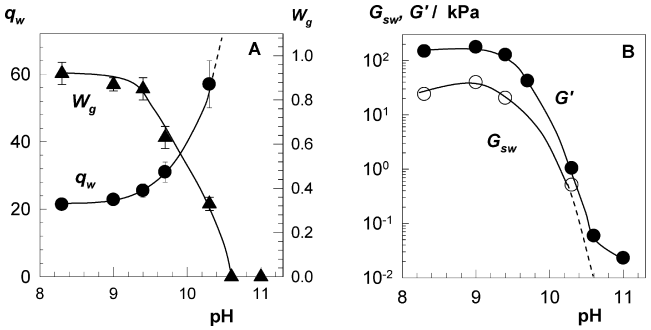

Figure 3. (A) Equilibrium swelling ratio q_w and the gel fraction W_g of fibroin hydrogels shown as a function of pH. q_w goes to infinity as pH approaches to 10.6, as represented by the dashed curve. (B) Elastic moduli G_{sw} of swollen hydrogels plotted against pH of the gelation solution. For comparison, the elastic moduli G' of hydrogels after 4 h of the reaction time are also replotted.

swollen hydrogels as 2 ± 0.5 nm, whereas it becomes 14 nm at pH 9.7 (See the Supporting Information for details.)

Secondary Structure of Fibroin Network Chains. Figure 4A shows X-ray profiles of freeze-dried hydrogels formed at various pH values. Silk fibroin before gelation (dotted curve in the Figure) exhibits a broad peak at ~22°, indicating an amorphous structure.[8] All hydrogels formed at pH <9.7 show a distinct peak at 20.9° and two minor peaks at 9.8 and 24.5°. These are the characteristic peaks of the β-sheet crystalline structure of silk fibroin corresponding to β-crystalline spacing distances of 4.3, 9.0, and 3.6 Å, respectively.[8,28] With increasing pH, that is, with decreasing modulus of the hydrogels, the main peak becomes broader and shifts toward higher angles, indicating decreasing crystallinity in the hydrogels. Because radiation-induced cross-linking may occur during the X-ray measurements, the secondary structure change of the fibroin was also assessed by FTIR. In the FTIR-ATR spectra of the fibroin samples, the amide I band was analyzed, representing the carbonyl stretching vibration of amide groups. The spectra of the freeze-dried hydrogels are shown in Figure 4B. The dotted curve representing the spectra of silk fibroin before gelation is characterized by a peak at 1640 cm^{-1}, indicating the presence of primarily random-coil and α-helix conformations.[20,48] After gelation, all samples display a main peak at 1620 cm^{-1}, which was assigned to β-sheet conformation.[48] In addition to the main peak, shoulders at 1660 and 1698 cm^{-1} are seen in the Figure, which can be assigned to α-helix and β-turn conformations, respectively.

dx.doi.org/10.1021/bm300006r | Biomacromolecules 2012, 13, 1122−1128

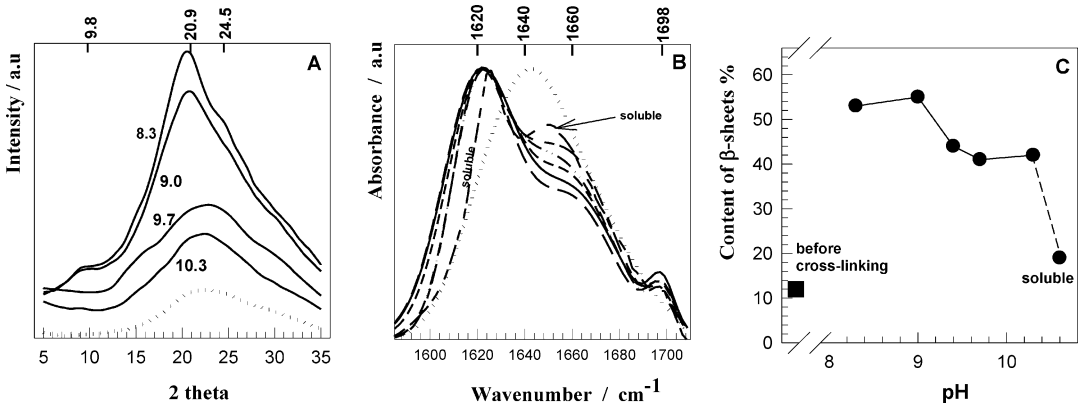

Figure 4. (A,B) X-ray diffraction (A) and FTIR spectra (B) of freeze-dried hydrogels. Data obtained by freeze-drying of silk fibroin solutions before gelation are also shown by the dotted curves. pH values are indicated in A, whereas in B, pH is 8.3 (solid curve), 9.0 (long dashed), 9.4 (short dashed), 9.7 (short–long), 10.3 (dashed-dotted-dotted), 10.6 (short–long–short), and 11.0 (dashed-dotted). Spectrum of the soluble hydrogel formed at pH 10.6 is indicated. (C) Content of β-sheets of silk fibroin network strands in freeze-dried hydrogels.

Increasing pH above 9.7 leads to increased intensity of the shoulder peak at 1660 cm^{-1}.

To estimate the conformation of the fibroin network chains, we carried peak separation of amide I band after baseline correction by selecting a Gaussian model for curve fitting. The peak positions were fixed at 1620, 1640, 1660, and 1698 cm^{-1}, representing β-sheet, random-coil, α-helix, and β-turn conformations, respectively (Figure S3 of the Supporting Information). The fraction of β-turns slightly increased from 1 ± 1 to 3 ± 1% upon gelation of fibroin solutions over the whole range of pH. The results of β-sheet contents collected in Figure 4C show that fibroin chains before gelation have 12 ± 2% β-sheet structures, whereas their contribution increases to 55% in the hydrogels formed between pH 8 and 9, which is close to the maximum crystallinity of silk fibroin. As the pH is further increased, this percentage decreases, and at pH 11 only 20% β-sheets were detected in soluble fibroin chains.

Mechanism of Gelation. The following scenario may explain the conformation transition in fibroin molecules in aqueous EGDE solutions (Figure 5). Previous works show that the driving force for the conformation transition in silk fibroin is the rearrangement of the hydrogen bonds between the fibroin chains.[8,49] The transition from random-coil to β-sheet structures depends on competition between breaking down of the original hydrogen bonds and the building up of the new ones between the silk fibroin chains,[23] which, in turn, depends on the backbone mobility. Both very high and very low degrees of segmental mobility inhibit the rearrangement of fibroin chains to form β-sheet structures. A conformation transition occurs easily if a limited degree of flexibility is provided to the fibroin chains, which can be achieved by increasing concentration or temperature and decreasing pH, addition of salts, nonsolvents, and so on.

In the present dilute fibroin solutions of concentration 4.2 w/v %, the chains move freely, making the formation of new hydrogen bonds between them difficult; therefore, as previously reported,[28] gelation requires very long times. However, as the fibroin molecules are connected each other via EGDE cross-links between the amino groups of arginine and lysine residues of hydrophilic chain blocks,[50,51] the branched chains can still move but not very freely, as compared with free chains (Figure 5). As a consequence, the nucleation and the growth of β-sheet structure through hydrophobic interactions of crystallizable blocks occur easily by the alignment of $(GAGAGS)_n$ amino acid

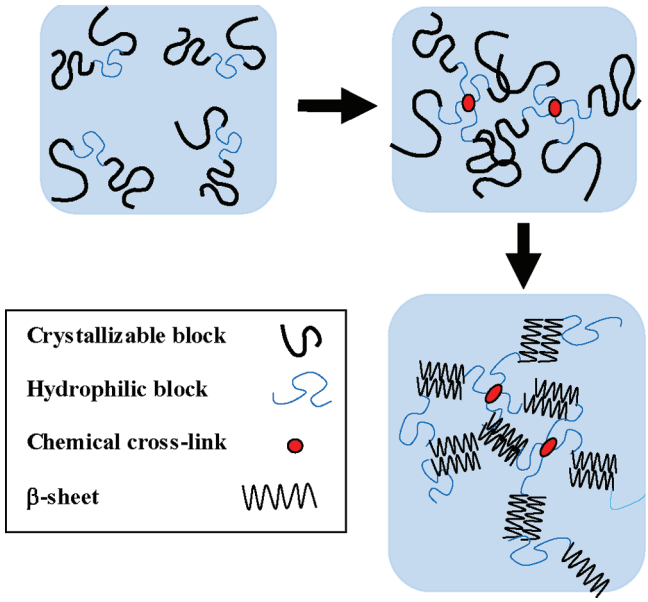

Figure 5. Cartoon demonstrating conformational changes and gelation of silk fibroin using EGDE cross-linker.

domains of individual chains. Therefore, introduction of chemical cross-links between the fibroin chains triggers the conformation transition and so facilitates the formation of fibroin gels. However, as the pH of the gelation solution is increased beyond 9.7, the osmotic pressure of the counterions on fibroin molecules causes chain expansion and thus inhibits the formation of β-sheets. This leads to a decrease in the modulus of fibroin hydrogels above pH 9.7.

To verify this hypothesis, we conducted stress-relaxation experiments on hydrogel samples just after their preparation. The relaxation modulus $G(t, \gamma_o)$ was monitored after application of a shear deformation of controlled amplitude γ_o for a duration of 100 s. It was found that the fibroin solution before gelation exhibits no strain hardening behavior; that is, $G(t, \gamma_o)$ does not increase with γ_o, implying that the un-cross-linked fibroin strands cannot align under strain due to the high degree of flexibility. In contrast, the loosely cross-linked hydrogels formed at pH >9.7 exhibited a significant degree of hardening. This supports the notion that by reducing the flexibility of the fibroin chains, one may facilitate the alignment

dx.doi.org/10.1021/bm300006r | Biomacromolecules 2012, 13, 1122–1128

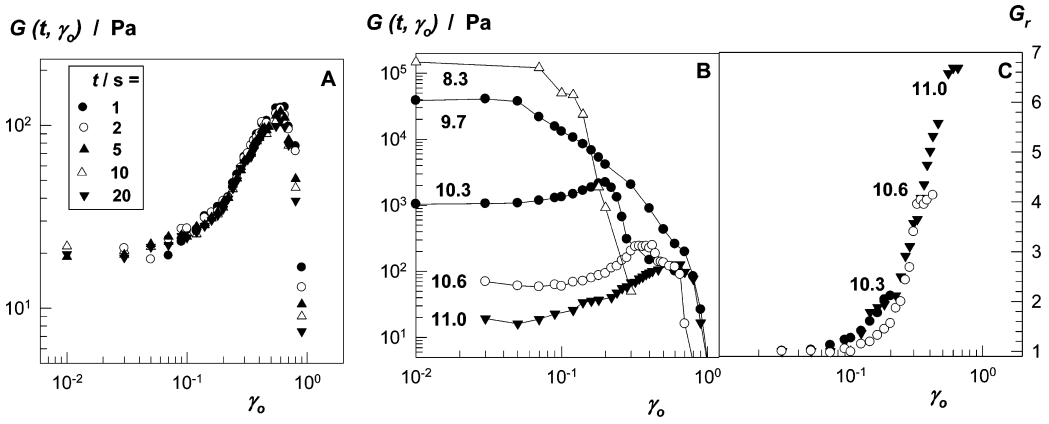

Figure 6. (A) Relaxation modulus $G(t, \gamma_o)$ of the hydrogels formed at pH 11.0 shown as a function of strain γ_o for various time scales t indicated. (B,C) $G(t, \gamma_o)$ (B) and the reduced modulus G_r (C) plotted against γ_o. For the sake of clarity, only data before the yield strain are plotted in C. t = 1 s. pH values indicated.

of the hydrophobic segments. Figure 6A shows the relaxation modulus $G(t, \gamma_o)$ of fibroin hydrogels formed at pH 11.0 as a function of strain γ_o for various time t. Independent of the time scale of experiments, fibroin hydrogels are in the linear regime; that is, the modulus is independent of strain for γ_o below 5%, whereas they exhibit strain hardening for γ_o between 5 and 60% before softening at higher strains. Similar plots were also obtained for other fibroin hydrogels prepared at pH >9.7. In Figure 6B,C, the modulus $G(t, \gamma_o)$ and the reduced modulus G_r normalized with respect to the modulus at zero strain are plotted against γ_o. High-modulus fibroin hydrogels with complete crystallinity exhibit no hardening behavior, whereas decreasing modulus simultaneously increases the extent of hardening. A maximum degree of hardening (700%) was observed in water-soluble hydrogels formed at pH 11.0. The results suggest that the applied strain contributes to the organization degree of the crystallizable amino acid domains in the fibroin network chains so that the modulus increases.

To elucidate the relative contribution of chemical (EGDE) and physical cross-links (β-sheet) to the effective cross-link density of fibroin hydrogels, we designed experiments to inhibit the chemical cross-linking reactions and simultaneously to promote the conformation transition of fibroin. Aqueous fibroin solutions are known to undergo conformation transitions more easily in acidic solutions because of the decrease in the repulsions among the chains facilitating intermolecular interactions and the formation of β-sheet structure. Therefore, gelation experiments were conducted near the isoelectric point (pI = 3.8 to 3.9) of silk fibroin by adjusting pH through the addition of acetic acid. At these pH values, EGDE does not react with the functional groups of fibroin so that one may expect formation of hydrogels with only β-sheet domains. Experiments conducted in the presence of 150% EGDE showed that the amine group content of fibroin as well as the dynamic moduli of the solutions remain unchanged up to 6 to 7 h, indicating that EGDE does indeed not react at a low pH. However, at longer times both G' and G'' rapidly increased and attained plateau values (Figure S5 of the Supporting Information). The limiting values of G' and G'' after 8 to 9 h were around 150 and 3 kPa, respectively, the same as those obtained at pH between 8.3 and 9.4 (Figure 2A). This means that the β-sheet structures acting as physical cross-links dominate over the interstrand EGDE cross-links in determining the elasticity of fibroin hydrogels.

CONCLUSIONS

Conformational transition of silk fibroin in the presence of EGDE as a cross-linker and resulting gelation were investigated in 4.2 w/v % aqueous fibroin solutions at 50 °C. The secondary structural change of the fibroin from random-coil to β-sheet was assessed by XRD and FTIR. Introduction of EGDE cross-links between the fibroin molecules decreases the mobility of the chains, which triggers the conformational transition and hence fibroin gelation in a short period of time. Dynamic rheological measurements show the formation of strong to weak hydrogels depending on the pH of the reaction solution. The elastic modulus of fibroin hydrogels formed between pH 8.3 to 9.7 is more than two orders of magnitude larger than the modulus of chemical or other biological gels. Although EGDE attacks the amino groups of fibroin and forms interstrand cross-links, β-sheets acting as physical cross-links dominate the elasticity of the hydrogels. Mechanical response of low-modulus fibroin hydrogels formed above pH 9.7 is highly nonlinear with strong strain hardening behavior (700%) arising from the alignment of the crystallizable amino acid segments.

ASSOCIATED CONTENT

Supporting Information

Calculation of the network mesh size in swollen fibroin hydrogels, pH of the reaction solution as a function of TEMED concentration, the calibration curve for the determination of the free amino groups on silk fibroin, typical ATR-FTIR spectrum and hidden peaks of a freeze-dried hydrogel sample, the elastic modulus G' during the cross-linking of silk fibroin at various EGDE %, and dynamic moduli versus time plots during the cross-linking of silk fibroin at various pH values. This material is available free of charge via the Internet at http://pubs.acs.org.

AUTHOR INFORMATION

Notes

The authors declare no competing financial interest.

ACKNOWLEDGMENTS

O.O. thanks Turkish Academy of Sciences (TUBA) for the partial support.

REFERENCES

(1) Vepari, C.; Kaplan, D. L. *Prog. Polym. Sci.* **2007**, *32*, 991.
(2) Vollrath, F.; Porter, D. *Polymer* **2009**, *50*, 5623.
(3) Hardy, J. G.; Romer, L. M.; Scheibel, T. R. *Polymer* **2008**, *49*, 4309.
(4) Zhou, C. Z.; Confalonieri, F.; Medina, N.; Zivanovic, Y.; Esnault, C.; Yang, T.; Jacquet, M.; Janin, J.; Duguet, M.; Perasso, R.; Li., Z. G. *Nucleic Acids Res.* **2000**, *28*, 2413.
(5) Sofia, S.; McCarthy, M. B.; Gronowicz, G.; Kaplan, D. L. *J. Biomed. Mater. Res.* **2001**, *54*, 139.
(6) Jin, H. J.; Fridrikh, S. V.; Rutledge, G. C.; Kaplan, D. L. *Biomacromolecules* **2002**, *3*, 1233.
(7) Jin, H. J.; Kaplan, D. L. *Nature* **2003**, *424*, 1057.
(8) Kim, U. J.; Park, J.; Li, C.; Jin, H. J.; Valluzzi, R.; Kaplan, D. L. *Biomacromolecules* **2004**, *5*, 786.
(9) Matsumoto, A.; Chen, J.; Collette, A. L.; Kim, U. J.; Altman, G. H.; Cebe, P.; Kaplan, D. L. *J. Phys. Chem. B.* **2006**, *110*, 21630.
(10) Magoshi, J.; Magoshi, Y.; Nakamura, S. Mechanism of Fiber Formation of Silkworm. In *Silk Polymers*; Kaplan, D., Adams, W. W., Farmer, B., Viney, C., Eds.; American Chemical Society: Washington, DC, 1994; pp 292−310.
(11) Knight, D. P.; Vollrath, F. *Naturwissenschaften* **2001**, *88*, 179.
(12) Chen, X.; Knight, D. P.; Vollrath, F. *Biomacromolecules* **2002**, *3*, 644.
(13) Terry, A. E.; Knight, D. P.; Porter, D.; Vollrath, F. *Biomacromolecules* **2004**, *5*, 768.
(14) Dicko, C.; Vollrath, F.; Kenney, J. M. *Biomacromolecules* **2004**, *5*, 704.
(15) Zong, X. H.; Zhou, P.; Shao, Z. Z.; Chen, S. M.; Chen, X.; Hu, B. W.; Deng, F.; Yao, W. H. *Biochemistry* **2004**, *43*, 11932.
(16) Dicko, C.; Kenney, J. M.; Knight, D.; Vollrath, F. *Biochemistry* **2004**, *43*, 14080.
(17) Magoshi, J. Biospinning (Silk Fiber Formation, Multiple Spinning Mechanisms). In *Polymeric Materials Encyclopedia*; Salamone, J. C., Ed.; CRC Press: New York, 1996; pp 667−679.
(18) Ochi, A.; Hossain, K. S.; Magoshi, J.; Nemoto, N. *Biomacromolecules* **2002**, *3*, 1187.
(19) Hossain, K. S.; Ochi, A.; Magoshi, J.; Nemoto, N. *Biomacromolecules* **2003**, *4*, 350.
(20) Chen, X.; Knight, D. P.; Shao, Z. Z.; Vollrath, F. *Biochemistry* **2002**, *41*, 14944.
(21) Zhou, L.; Chen, X.; Shao, Z. Z.; Zhou, P.; Knight, D. P.; Vollrath, F. *FEBS Lett.* **2003**, *554*, 337.
(22) Chen, X.; Shao, Z. Z.; Knight, D. P.; Vollrath, F. *Acta Chim. Sin.* **2002**, *60*, 2203.
(23) Chen, X.; Shao, Z. Z.; Knight, D. P.; Vollrath, F. *Proteins: Struct., Funct., Bioinf.* **2007**, *68*, 223.
(24) Servoli, E.; Maniglio, D.; Motta, A.; Migliaresi, C. *Macromol. Biosci.* **2008**, *8*, 827.
(25) Leisk, G. G.; Lo, T. J.; Yucel, T.; Lu, Q.; Kaplan, D. L. *Adv. Mater.* **2010**, *22*, 711.
(26) Winkler, S.; Kaplan, D. L. *Rev. Mol. Biotechnol.* **2000**, *74*, 85.
(27) Um, I. C.; Kweon, H. Y.; Lee, K. G.; Park, Y. H. *Int. J. Biol. Macromol.* **2003**, *33*, 203.
(28) Ayub, Z. H.; Arai, M.; Hirabayashi, K. *Biosci. Biotechnol. Biochem.* **1993**, *57*, 1910.
(29) Lu, X.; Xu, Y.; Zheng, C.; Zhang, G.; Su, Z. *J. Chem. Technol. Biotechnol.* **2006**, *81*, 767.
(30) Amiya, T.; Tanaka, T. *Macromolecules* **1987**, *20*, 1162.
(31) Topuz, F.; Okay, O. *Macromolecules* **2008**, *41*, 8847.
(32) Topuz, F.; Okay, O. *Biomacromolecules* **2009**, *10*, 2652.
(33) Xu, J.; Tseng, Y.; Wirtz, D. J. *J. Biol. Chem.* **2000**, *275*, 35886.
(34) Gardel, M. L.; Shin, J. H.; MacKintosh, F. C.; Mahadevan, L.; Matsudaira, P.; Weitz, D. A. *Science* **2004**, *304*, 1301.
(35) Gardel, M. L.; Kasza, K. E.; Brangwynne, C. P.; Liu, J.; Weitz, D. A. *Methods Cell Biol.* **2008**, *89*, 487.
(36) Shah, J. V.; Janmey, P. A. *Rheol. Acta* **1997**, *36*, 262.
(37) Orakdogen, N.; Erman, B.; Okay, O. *Macromolecules* **2010**, *43*, 1530.
(38) Habeeb, A. F. S. A. *Anal. Biochem.* **1966**, *14*, 328.
(39) Hermanson, G. *Bioconjugate Techniques*; Academic Press: San Diego, CA, 1996; pp 112−113.
(40) Shimura, K.; Kikuchi, A.; Katagata, Y.; Ohotomo, K. *J. Seric. Sci. Jpn.* **1982**, *51*, 20.
(41) Sayil, C.; Okay, O. *Polymer* **2001**, *42*, 7639.
(42) Gundogan, N.; Melekaslan, D.; Okay, O. *Macromolecules* **2002**, *35*, 5616.
(43) Lee, K. J.; Lee, D. K.; Kim, Y. W.; Kim, J. H. *Eur. Polym. J.* **2007**, *43*, 4460.
(44) Nguyen, T. T.; Raupach, M.; Janik, L. J. *Clays Clay Miner.* **1987**, *35*, 60.
(45) Li, M; Tao, W.; Lu, S.; Kuga, S. *Int. J. Biol. Macromol.* **2003**, *32*, 159.
(46) Storm, C.; Pastore, J. J.; MacKintosh, F. C.; Lubensky, T. C.; Janmey, P. A. *Nature* **2005**, *435*, 191.
(47) Yan, H.; Saiani, A.; Gough, J. E.; Miller, A. F. *Biomacromolecules* **2006**, *7*, 2776.
(48) Mo, C.; Holland, C.; Porter, D.; Shao, Z.; Vollrath, F. *Biomacromolecules* **2009**, *10*, 2724.
(49) Hu, X.; Lu, Q.; Kaplan, D. L.; Cebe, P. *Macromolecules* **2009**, *42*, 2079.
(50) Shiozaki, H.; Tanaka, Y. *Makromol. Chem.* **1972**, *152*, 217.
(51) Shiozaki, H.; Tsukada, M.; Gotah, Y.; Kasai, N.; Freddi, G. *J. Appl. Polym. Sci.* **1994**, *52*, 1037.